Simulation of the Self-Assembly of Symmetric Triblock Copolymers in Dilute Solution

Yongmei Wang and Wayne L. Mattice*

Institute of Polymer Science, University of Akron, Akron, Ohio 44325-3909

Donald H. Napper

Department of Physical and Theoretical Chemistry, School of Chemistry, The University of Sydney, Sydney, New South Wales 2006, Australia

Received February 13, 1992; Revised Manuscript Received April 29, 1992

ABSTRACT: The simulation of the self-assembly of symmetric triblock copolymers, A_{N_A}–B_{N_B}–A_{N_A}, has been performed on a cubic lattice. In all of these simulations the pairwise energy of interaction of A with B (E_{AB}) is identical with the pairwise interaction of A with a void, or solvent (E_{AS}), and all other pairwise interactions are zero. The ratio of the number of observations of single dispersed chains that form internal loops to the number that have no interaction between their terminal blocks is studied for its implications for the influence of loop formation on the self-assembly of the system. As $N_A \to 1$ the loop formation approaches that predicted by Jacobson and Stockmayer, but the entropic penalty associated with loop formation decreases as N_A increases. This result has strong implications for the structures formed upon self-assembly of A_{N_A}–B_{N_B}–A_{N_A}. The type of aggregation observed when $E_{AB} = E_{AS} > 0$ depends on whether the conditions correspond to weak or strong segregation. At weak segregation, the change in volume fraction of A_{N_A}–B_{N_B}–A_{N_A} produces two transitions. The first transition produces a very loosely organized micelle-like structure, and the second transition, at higher concentration, produces an enormous aggregate that we interpret as signifying separation into a gel-like macrophase. At strong segregation the system assembles into a micelle with a well-organized classical core–shell structure. The transition to a gel-like macrophase is suppressed.

Introduction

Triblock copolymers, A_{N_A}–B_{N_B}–A_{N_A}, exhibit interesting phenomena in selective solvents which interact preferentially with the beads of B in the internal block. Several phenomena can be envisioned to occur. The copolymers could assemble into micelles where the terminal blocks of A form the core and the middle blocks of B form the corona.[1] This structure would require the formation of a loop by the central block of B if both of the terminal blocks of A are to be part of the core of the same micelle. The triblock copolymers could also assemble into a gel-like network where small aggregates are bridged by extended soluble blocks of B. In this structure the two terminal blocks of A can be located in the cores to two different small aggregates. Another possibility is that the triblock copolymers would participate in intramolecular association, resulting in the formation of "hairpins". When compared with the structures accessible to A_{N_A}–B_{N_B}, a richer variety of structures could in principle exist for A_{N_A}–B_{N_B}–A_{N_A}.

In the early literature on block copolymers, there is some disagreement about whether A_{N_A}–B_{N_B}–A_{N_A} with sticky ends can assemble into micelles.[2-5] On the basis of their calculations and some of the experimental results,[5] ten Brinke and Hadziioannou concluded that the loss of the entropy of the coronal loops would preclude the formation of micelles in most instances.[6] Recent experiments by Balsara et al.[1] have convincingly shown the occurrence of aggregation. They claimed that ten Brinke and Hadziioannou overestimated the entropic penalty involved in the placement of both terminal blocks of A_{N_A}–B_{N_B}–A_{N_A} in the same core and concluded that micelles could indeed form. The approaches by both groups considered only those conformations of A_{N_A}–B_{N_B}–A_{N_A} that place both terminal blocks in the same core. Here we present the results of simulations of multimolecular systems of A_{N_A}–B_{N_B}–A_{N_A} in selective solvents. These simulations do not impose any preconceived notions about the conformations accessible to the chains. They provide the opportunity to easily study the structures formed upon the self-assembly of A_{N_A}–B_{N_B}–A_{N_A}.

Earlier we presented preliminary results from the simulation of 20 molecules of $A_5B_{10}A_5$.[7] These preliminary results showed the existence, under appropriate conditions, of the various types of structure that have been envisioned. Here we extend those preliminary studies to larger systems, which allow the simulation of more chains and longer chains. In the case of diblock copolymers in selective solvents, the simulation shows the onset of micellization clearly, and the cmc (critical micelle concentration) can be easily extracted from the results.[8] In the case of triblock copolymers in selective solvents, we will show that the micelles with the classical core–shell structure can form, but only under conditions of relatively strong segregation. When the segregation is weak, the chains do not form the loops required for the placement of both terminal blocks in a single core. Instead there is successive aggregation of the insoluble terminal blocks, which leads ultimately to a macrophase separation in the system. We will also show that the estimation of the free energy of loop formation postulated by ten Brinke and Hadziioannou[6] is applicable to these molecules, but the prefactor they denote by β does not always have a value close to 1 as they assumed. Rather, the value of β depends on the value of N_A and becomes much less than one as N_A increases. According to ten Brinke and Hadziioannou,[6] micellization would be possible when the value of β falls below some critical value. Their results will lead to a correct prediction of the behavior of A_{N_A}–B_{N_B}–A_{N_A} when one realizes that β can, under appropriate circumstances, be much smaller than one.

Method

The methodology employed in the simulation is essentially the same as that used in recent work.[7-9] The periodic box used in the simulations is a cubic lattice of dimensions 44 × 44 × 44. Every chain of the symmetric triblock copolymer, A_{N_A}–B_{N_B}–A_{N_A}, has the same size, where each block contains N_A beads of A or N_B beads of B. No lattice

0024-9297/92/2225-4073$03.00/0

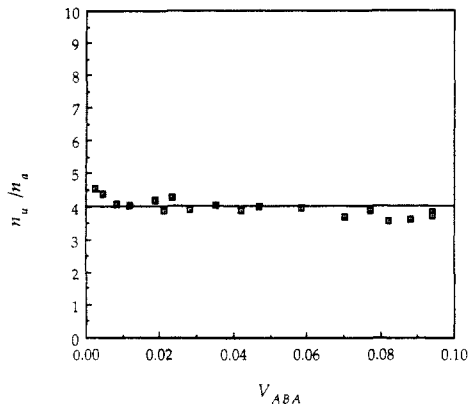

Figure 1. Behavior of n_u/n_a as a function of the volume fraction of A_5–B_{10}–A_5 when $\chi/k = 0.25$.

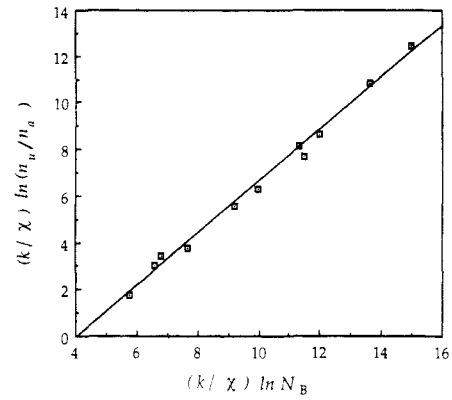

Figure 2. Behavior of the ratio of unassociated and intramolecularly associated dispersed chains in simulations of A_5–B_{N_B}–A_5 when N_B and χ are varied. The straight line has a slope of 1.1.

site can be occupied by more than one bead. Vacant sites are considered to be occupied by solvent, S. Reptation and the Metropolis rules are used to convert one replica into another. The pairwise interaction, $E_{AB} = E_{AS}$, is applied whenever A has a nonbonded B, or a vacant site S, as a nearest neighbor. All remaining pairwise interactions are taken to be zero. No lattice site can be occupied by more than one bead. The reduced interaction energy, $E_{AB}/k_BT = E_{AS}/k_BT$, will be denoted by χ/k, where k is a lattice constant.[8] This χ is equivalent to the Flory–Huggins parameters, $\chi_{AB}^{F\text{-}H} = \chi_{AS}^{F\text{-}H}$. The numerical value of k is about 3.2 for the system used here.[8]

Interchain aggregation is defined to occur whenever a bead of A on one chain is a nearest neighbor of a bead of A on another chain. Intrachain aggregation is defined to occur when a bead of A in one block has a bead of A from the other block of the same molecule as a nearest neighbor.

Results and Discussion

Single Dispersed Chains. Here we divide all of the conformations of an individually dispersed chain of A_{N_A}–B_{N_B}–A_{N_A} into two groups. One group has intramolecular association of the two terminal blocks, and in the other group the terminal blocks do not interact with one another. In the simulations, the numbers of observations of chains that fall into the first and the second groups are denoted by n_a and n_u, respectively. The value of n_u/n_a is observed to be independent of the volume fraction of the copolymer, V_{ABA}, defined as

$$V_{ABA} = \frac{N_C(2N_A + N_B)}{L^3} \tag{1}$$

where N_C denotes the number of chains in the periodic box and L^3 is the number of sites in the box. In all of the simulations described here, $L = 44$. Figure 1 depicts the value of n_u/n_a as a function of V_{ABA} for A_5–B_{10}–A_5 when $\chi/k = 0.25$. As we will show below, the range of V_{ABA} covered in Figure 1 includes the cmc and a second transition that produces a structure much larger than the micelle. Neither of these transitions has any effect on the value of n_u/n_a. The value of n_u/n_a is determined entirely by the architecture of the individual chain and the interaction energy.

Since ten Brinke and Hadziioannou[6] and Balsara et al.[1] have given two different estimations for the free energy of loop formation, it is interesting to compare the values of n_u/n_a deduced from the simulations with their theoretical predictions. The ratio of the populations of associated and unassociated states can be written by analogy to the equilibrium constant in a chemical reaction,

$$\Delta G = -k_BT \ln (n_a/n_u) \tag{2}$$

where ΔG is the standard free energy difference between the associated state and the unassociated state. The contribution to ΔG from the enthalpic term was taken to be proportional to $-\chi k_BTN_A$ for the self-associated dispersed chain. The entropic term arises from loop formation. ten Brinke and Hadziioannou give the free energy of loop formation as[6]

$$F_{loop} = (3/2)\beta k_BT \ln N_B \tag{3}$$

Here the parameter denoted by β allows for any deviations of the entropy of loop formation from the prediction of the model of Jacobson and Stockmayer.[10] The Jacobson–Stockmayer result is obtained when $\beta = 1$. Applied to the system in the simulation, we have

$$-k_BT \ln (n_a/n_u) = -\chi^{F\text{-}H}k_BT\alpha N_A + (3/2)k_BT\beta \ln N_B \tag{4}$$

where α is a constant that permits deviation of the enthalpic term from the approximation. If N_A is fixed, the enthalpic term only contains the variable $\chi^{F\text{-}H}$. In the simulation, $\chi^{F\text{-}H}$ can be replaced with χ/k. Thus a plot of $\chi^{-1} \ln (n_u/n_a)$ vs $\chi^{-1} \ln N_B$ should yield a straight line with a slope equal to $(3/2)\beta$. Figure 2 depicts the plot for the case where $N_A = 5$. The points are the results from 11 simulations that employ different values of χ and N_B. The data describe a straight line with a slope of 1.1. That slope implies a value of β of about 0.7. Therefore, at $N_A = 5$, the results from the simulations have a form that is consistent with the prediction from eq 4.

A more informative test of eq 4 is provided by a more extensive series of simulations carried out with different values of N_A. The plots of these results, obtained with different numerical assignments for N_A, also yield straight lines. The slopes and intercepts of these lines decrease as N_A increases, as is shown in Figure 3. The values of β extracted from these straight lines are depicted in Figure 4 as a function of N_A. When N_A has the value of one, the straight line specifies a value of β that is only slightly larger than one. The expectation value of β from the macrocyclization theory of Jacobson and Stockmayer is one.[10] However, that result does not incorporate the influence of excluded volume. Incorporation of that effect should produce a value of β that is slightly larger than one. Therefore we judge the results when $N_A = 1$ as being in reasonable agreement with the expectation from the macrocyclization theory of Jacobson and Stockmayer.[10]

The decrease in β with an increase in N_A arises because the increase in the sizes of the terminal blocks means that more conformations of the central block can produce an

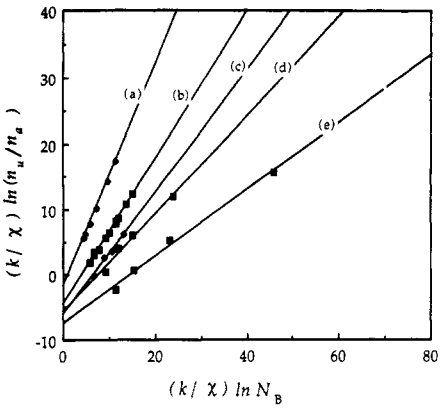

Figure 3. Behavior of the ratio of unassociated and intramolecularly associated dispersed chains in simulations of A_{N_A}–B_{N_B}–A_{N_A} when N_B and χ are varied at different values for N_A. The values of N_A are 1, 5, 8, 10, and 15 for curves a, b, c, d, and e, respectively.

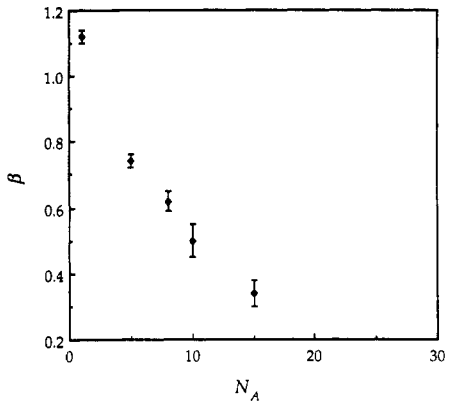

Figure 4. Dependence of β on N_A for A_{N_A}–B_{N_B}–A_{N_A}.

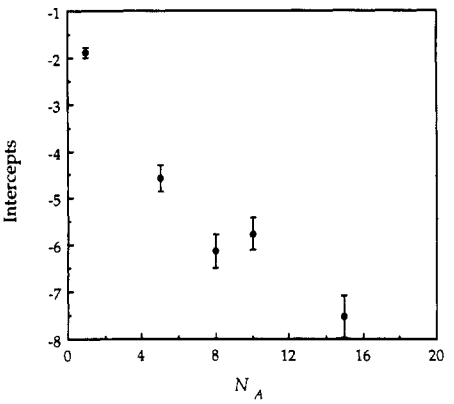

Figure 5. Dependence of the intercepts in Figure 3 on N_A.

interaction between beads in the terminal blocks. Therefore the reduction in entropy of B_N becomes less severe as N_A increases. Only in the limit where $N_A \to 1$ do we recover a value close to the Jacobson–Stockmayer result, $\beta = 1$.

According to eq 4, the intercepts in Figure 3 are equal to $-\alpha N_A$. The appearance of α in this term adjusts the enthalpic contribution. The nature of the interconnection between the value of α and the size of the terminal blocks can be assessed using the results from the simulations. Figure 5 plots the intercepts from Figure 3 as a function of N_A. The curvature apparent in Figure 5 suggests that the effective value of α decreases as N_A increases. The initial slope in this figure is consistent with a value of α that approaches 1 as $N_A \to 1$. The dependence of α on N_A can be rationalized as follows. In the limit of $N_A \to 1$, an isolated chain has exactly N_A contacts between beads of A in one block and beads of A in the other block when that chain forms an intramolecular association. However, as

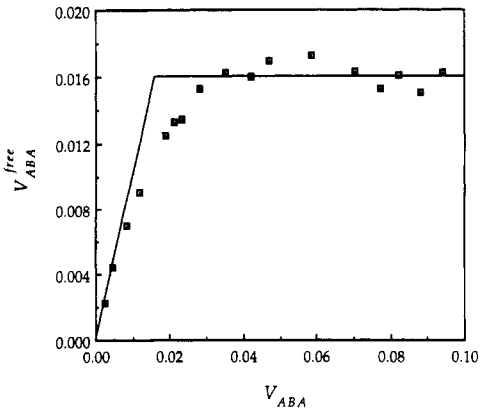

Figure 6. Relationship between the volume fraction of free chains, V_{ABA}^{free}, and the total volume fraction, V_{ABA}, for A_5–B_{10}–A_5 when $\chi/k = 0.25$.

N_A increases, there are more conformations where the chain still has an intramolecular association, but that association does not produce exactly N_A contacts of beads of A from different blocks. The disorder in the two blocks will instead place many of the beads of A in positions where they cannot participate in contacts with beads of A from the block at the other end of the chain. Hence the average number of A–A contacts between the two blocks will fall below N_A as N_A increases. In terms of eq 4, the value of α decreases as N_A increases.

An attempt was made to apply the free energy expression given by Balsara et al.,[1] but their form does not conform to the data generated in the simulations. Their form is really only applicable in considering the chains inside micelles, and it is not applicable to the formation of "hairpins" by isolated chains. Thus we are not able to confirm whether their form is correct. However, their expression does predict a smaller penalty for loop formation compared to ten Brinke and Hadziioannou[6] with $\beta = 1$.

Aggregation under Conditions of Weak Segregation. Figure 6 depicts the volume fraction of free chains, V_{ABA}^{free}, as a function of the volume fraction of all chains, V_{ABA}. The copolymers have $N_A = 5$, $N_B = 10$, and $\chi/k = 0.25$. The figure contains two straight lines, one of which has a slope of one and passes through the origin and the other of which has a slope of zero and an intercept of 0.016 on the vertical axis. These two straight lines provide a reasonably good approximation to the data from the 17 simulations. The transition of V_{ABA} in Figure 6 does not have an effect on the ratio of unaggregated and self-aggregated dispersed chains because there is no disturbance in the data near $V_{ABA} = 0.016$ in Figure 1. Data presented previously[8] for a diblock copolymer, A_{10}–B_{10}, also with $\chi/k = 0.25$, show a very similar transition where micellization occurs. The plateau value for V_{AB}^{free} for the diblock copolymer occurred at a slightly smaller value, 0.012. Thus the cmc for the diblock copolymer is slightly smaller than the cmc for the triblock copolymer under these conditions.

A more dramatic difference between the behavior of the diblock and triblock copolymers is revealed by following the average sizes of the aggregates. The dimensionless measure used for this purpose is M_w/M_0, where M_w denotes the usual weight-average molecular weight of the micelle and M_0 denotes the mass of one molecule of the block copolymer. In the case of the diblock copolymer, M_w/M_0 shows an increase at the value of V_{AB} that corresponds to the cmc. In contrast, with the triblock copolymer there is a relatively modest increase in M_w/M_0 at the value of V_{ABA} that corresponds to the cmc, followed

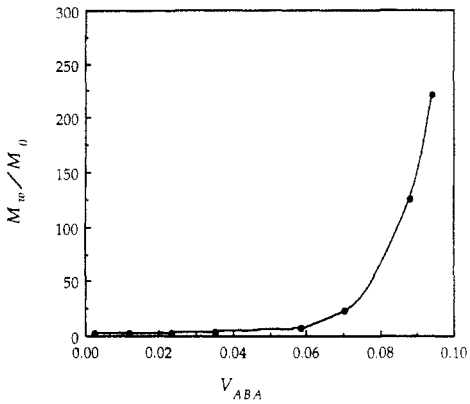

Figure 7. M_w/M_0 as a function of V_{ABA} for A_5–B_{10}–A_5 when $\chi/k = 0.25$.

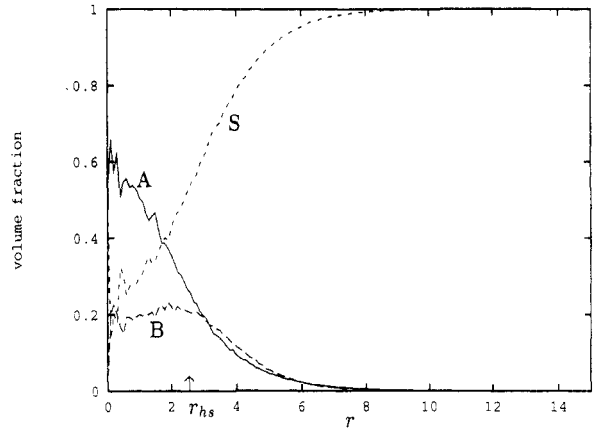

Figure 8. Volume fractions of A, B, and solvent versus the radial distance r in an aggregate of A_5–B_{10}–A_5 with M_w/M_0 around 14, $V_{ABA} = 0.04$, and $\chi/k = 0.25$.

by a much more dramatic increase at higher concentrations, as shown in Figure 7. The large increase in M_w/M_0 at $V_{ABA} > 0.06$ in Figure 7 does not affect the concentrations of free chains (Figure 6) nor the ratio of unaggregated to self-aggregated free chains (Figure 1).

Figure 8 presents the distributions of A, B, and solvent (voids) about the center of mass of a typical aggregate with M_w/M_0 of about 14, which is found at V_{ABA} near 0.04. This concentration is above the cmc (Figure 6) but below the onset of the formation of aggregates with very large values of M_w/M_0 (Figure 7). The three curves in Figure 8 present the volume fractions of the three components in successive spherical shells, with the sum of these three volume fractions being one in every spherical shell. The horizontal axis is the distance of the spherical shell from the center of mass of the aggregate, expressed in units of the lattice spacing. The small arrow in Figure 7 indicates the value of r_{hs}, which denotes the radius of the most compact sphere that can contain all of the beads of A in the aggregate. With an aggregate containing n_{ag} blocks of A

$$r_{hs} = \left(\frac{3n_{ag}N_A}{4\pi}\right)^{1/3} \tag{5}$$

For a classic core–shell model of a spherical micelle, $V_A = 1$ when $r < r_{hs}$ and $V_A = 0$ when $r > r_{hs}$. Figure 8 shows that the aggregate approximates this simple model only in that the core is rich in A ($V_A > V_B$ when $r < r_{hs}$ and $V_A > V_S$ when $r < (2/3)r_{hs}$). Important departures from the simple model are evident in the presence of a significant amount of B and solvent near the center of mass of the aggregate and in the presence of a large amount of A at $r_{hs} < r < 2r_{hs}$. Evidently the free energy associated with

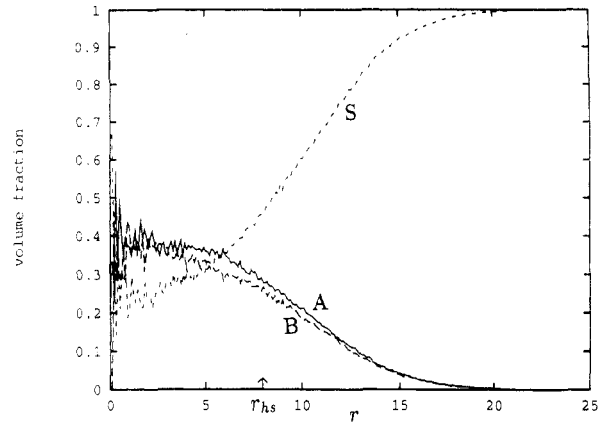

Figure 9. Volume fractions of A, B, and solvent versus r in an aggregate of A_5–B_{10}–A_5 with M_w/M_0 around 425, $V_{ABA} = 0.1$, and $\chi/k = 0.25$.

loop formation is too large to permit all of the blocks of B to adopt conformations that will place both terminal blocks of A in the core and confine the block of B to the region of the corona, as expected.[11] This result is further confirmed by the dimensionless characteristic ratio, defined for present purposes as

$$C = \frac{\langle r^2 \rangle}{(2N_A + N_B - 1)l^2} \tag{6}$$

where $\langle r^2 \rangle$ denotes the mean square end-to-end distance for A_{N_A}–B_{N_B}–A_{N_A} and l denotes the length of the bond between beads. The value of C is 1.45 for the chains of A_{N_A}–B_{N_B}–A_{N_A} that participate in the formation of this structure. This result is nearly identical with the value, 1.50, expected for a long unperturbed chain with the bond angles and dihedral angles appropriate to the chains on the lattice. Clearly "hairpins" are not a dominant conformation.

The large aggregates formed at $V_{ABA} > 0.06$ have a much different internal structure from the smaller aggregates described in Figure 8. Figure 9 presents the distribution functions for a large aggregate that contains 425 blocks of A, formed by A_5–B_{10}–A_5 when $V_{ABA} = 0.1$. Here there is very little difference in the volume fractions of A and B at any distance from the center of mass. Furthermore, there is no evidence for a rapid change in the volume fractions of either A or B as one passes through the region where $r = r_{hs}$. The value of r_{hs} for this large structure is 8 in lattice units, and therefore $r_{hs} > N_A$. Even if the blocks of A were fully extended, they could not span the distance from the center of mass of the aggregate to the position where $r = r_{hs}$. The individual chains involved in the formation of this large aggregate have a slightly larger value of C, 1.58, then the unperturbed chain. The chains in the large aggregate are slightly more extended than those involved in the formation of the smaller aggregate described in Figure 8. This large structure we interpret as the onset of macrophase separation.

Under these conditions of weak segregation, the triblock copolymer initially aggregates into a rather poor approximation to a classic spherical micelle. At higher concentrations, aggregation of the blocks of A leads to macrophase separation.

Aggregation under Conditions of Strong Segregation. A distinctly different behavior is obtained under conditions of stronger segregation. Here we impose those conditions by retaining the value of χ/k and doubling the sizes of N_A and N_B. This simulation of A_{10}–B_{20}–A_{10} produces micelles with varying sizes. Figure 10 depicts

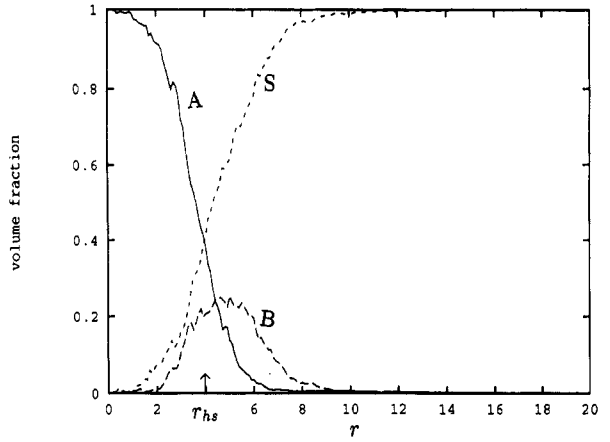

Figure 10. Volume fractions of A, B, and solvent versus r in an aggregate of A_{10}–B_{20}–A_{10} with M_w/M_0 around 26, V_{ABA} = 0.14, and χ/k = 0.25.

the internal structure of a typical micelle found in the system when V_{ABA} = 0.14. This micelle, which contains beads from 26 blocks of A, has an internal structure that is much closer to the expectation for a classic spherical micelle with a core–shell structure than did either of the structures formed by A_5–B_{10}–A_5. The value of V_A is very close to one for most of the region where $r < r_{hs}$, and it falls precipitously to a very small value as r rises above r_{hs}. The beads of B prefer the region of the corona, where r is slightly larger than r_{hs}. Most of the chains that are involved in this aggregate adopt the conformation of a loop, thereby placing both of their terminal blocks in the core. That fact is also reflected in the value of C, which is about 1.08 here, and thus much smaller than the unperturbed value of 1.50. Therefore the two terminal blocks are placed in the same core, and the blocks of B are confined to the coronal region.

It is clear from the results of these simulations that symmetric triblock copolymers can form micelles in media that interact preferentially with the internal block. The micelles can have a structure reminiscent of a classic core–shell structure under conditions of relatively strong segregation. Aggregates with less specific structures, and macrophase separation, are preferred to the classic core–shell micelle under conditions of weaker segregation.

ten Brinke and Hadziioannou indicated that there is a value of β above which micelles will not form.[6] Their treatment assumed that $\beta = 1$, which was above the critical value of β for formation of micelles under their specific conditions, and therefore they concluded that micelles would not form in most cases. Our results (Figure 4) show that β can become much smaller than 1 when N_A is large. The β value we have obtained here for intramolecular association represents an upper bound for chains involved in the self-assembly into micelles. It is anticipated that values of β would be smaller for most cases of the formation of micelles. Thus micelles do form under these conditions (and would have been predicted by the approach adopted by ten Brinke and Hadziioannou[6] had they realized that β might become quite small under these conditions).

Balsara et al.[1] adopted a different form for the loop formation, with the main difference being in the prefactor. Their formalism would appear to correspond to a value of β of about 0.33. At such small values of β, the simulations show the formation of micelles, and therefore it is not surprising the Balsara et al. predict the formation of micelles by symmetric triblock copolymers. Nevertheless, our data for the ratio of unaggregated to self-aggregated free chains is fitted better by the formalism used by ten Brinke and Hadziioannou.

The concentration of solvent in the core of a micelle may depend on the strength of the segregation, as shown by comparison of Figures 8 and 10. At strong segregation, the core will contain little solvent. Under these conditions, the dynamics of the exchange of chains between the micelle and the population of free chains may be strongly temperature dependent if the system is examined in the vicinity of the glass transition temperature for the insoluble block. This effect has recently been observed for diblock copolymers of polystyrene and poly(oxyethylene), using samples in which each chain contains either a Förster donor or a Förster acceptor at the junction between the two blocks.[12]

Conclusion

A controversy over the ability of symmetric triblock copolymers to self-assemble into micelles when the terminal blocks are in a poor solvent has been partially resolved. Only under conditions of relatively strong segregation does the self-assembly lead to a micelle with the classical core–shell structure. Under conditions of weak segregation, two transitions are observed as the volume fraction of copolymers increases. The first transition produces a very loosely organized micelle-like structure, and the second transition produces an enormous aggregate that we interpret as signifying separation into a gel-like macrophase.

Acknowledgment. This research was supported by National Science Foundation Grants DMR 89-14502 and INT 90-14836 and by the Australian Department of Industry, Technology, and Commerce.

References and Notes

(1) Balsara, N. P.; Tirrell, M.; Lodge, T. P. *Macromolecules* **1991**, *24*, 1975.
(2) Krause, S. *J. Phys. Chem.* **1964**, *68*, 1948.
(3) Tanaka, T.; Kotaka, T.; Inagaki, H. *Polym. J.* **1972**, *3*, 327.
(4) Kotaka, T.; Tanaka, T.; Hattori, M.; Inagaki, H. *Macromolecules* **1978**, *11*, 138.
(5) Tang, W. T.; Hadziioannou, G.; Cotts, P. J.; Smith, B. A.; Frank, C. W. *Polym. Prepr. (Am. Chem. Soc., Div. Polym. Chem.)* **1986**, *27* (2), 107.
(6) ten Brinke, G.; Hadziioannou, G. *Macromolecules* **1987**, *20*, 486.
(7) Rodrigues, K.; Mattice, W. L. *Polym. Bull.* **1991**, *25*, 239.
(8) Wang, Y.; Mattice, W. L.; Napper, D. H. *Langmuir*, submitted.
(9) Rodrigues, K.; Mattice, W. L. *J. Chem. Phys.* **1991**, *94*, 761.
(10) Jacobson, H.; Stockmayer, W. H. *J. Chem. Phys.* **1950**, *18*, 1600.
(11) Rodrigues, K.; Mattice, W. L. *Langmuir* **1992**, *8*, 456.
(12) Wang, Y.; Balaji, R.; Quirk, R. P.; Mattice, W. L. *Polym. Bull.*, in press.